Am J Transl Res 2019;11(5):2641-2656
www.ajtr.org /ISSN:1943-8141/AJTR0090117

Original Article

Bone regeneration using injectable poly (γ-benzyl-L-glutamate) microspheres loaded with adipose-derived stem cells in a mouse femoral non-union model

Zhongyue Huang[1*], Huijie Gu[1*], Xiaofan Yin[1*], Long Gao[2], Kunxi Zhang[2], Yiming Zhang[1], Jun Xu[1], Liang Wu[1], Jingbo Yin[2], Lei Cui[3,4]

[1]Department of Orthopedics, Minhang Hospital, Fudan University, Shanghai 201199, China; [2]Department of Polymer Materials, Shanghai University, Shanghai 200444, China; [3]Department of Plastic Surgery, Beijing Shijitan Hospital Affiliated to Capital Medical University, Beijing 100038, China; [4]Department of Orthopedics, Shanghai Tongji Hospital, Tongji University School of Medicine, Shanghai 200065, China. [*]Equal contributors.

Received December 19, 2018; Accepted March 11, 2019; Epub May 15, 2019; Published May 30, 2019

Abstract: Microspheres have gained immense popularity in bone tissue engineering because of their unique properties as injectable scaffolds for bone tissue regeneration. Herein, we evaluated the feasibility of using poly (γ-benzyl-L-glutamate) (PBLG) microspheres for bone engineering by examining the attachment, proliferation, and osteogenic differentiation of adipose-derived stem cells (ASCs) *in vitro* and the use of PBLG microspheres in healing non-union *in vivo*. Scanning electron microscopy and fluorescent 3, 30-dioctadecyloxacarbocyanine perchlorate-labeling were performed to study the attachment and growth of ASCs to the PBLG microspheres, and a DNA assay was performed to quantify cell proliferation with time. Osteogenic differentiation of ASCs cultured on the PBLG microspheres was assessed by determining alkaline phosphatase expression and extracellular calcium deposition, which was further confirmed by real-time polymerase chain reaction for osteogenesis-related genes. Femoral non-union were created in mouse models and filled with ASCs/PBLG microspheres *in vivo*. The results showed that ASCs attached, spread, and showed good osteogenic differentiation on the PBLG microspheres *in vitro*. Moreover, the ASCs/PBLG microspheres could repair the mouse femoral non-union *in vivo*. Thus, PBLG microspheres have good biocompatibility and cytocompatibility and are potentially useful as an injectable scaffolds for bone tissue engineering.

Keywords: Microspheres, poly (γ-benzyl-L-glutamate), adipose-derived stem cells, osteogenic differentiation, bone regeneration

Introduction

Delayed fracture healing and nonunion occurs in up to 10% of all fractures, and remains a substantial clinical problem [1]. Most hypertrophic nonunions can be well treated with stable osteosynthesis, while the treatment of atrophic nonunions is often difficult and highly challenging [2]. Atrophic nonunions are multifactorial, including different bones, fracture site, initial degree of bone loss, time elapsed since injury, extent of soft-tissue injury, as well as a host of patient factors such as smoking, diabetes, and other systemic diseases [3]. A deficient osteogenesis was considered as the main cause [4]. The fresh autogenous grafts are considered as a gold standard in the treatment of nonunions [1]. However, significant problems, such as the size limitations of autogenous bone grafts, problems with chronic pain at the donor site, and complications of the procedures, restrict its clinical use [3, 5]. Development of bone tissue engineering provides a novel approach for bone regeneration through the combination of scaffolds, seed cells, and biologically active molecules. The tissue engineering bone graft contains living cells that can produce osteoinductive, osteoconductive, and osteogenic properties.

In the duration of recent decades, microspheres have been paid much attention to in bone tissue engineering because of their unique properties as injectable scaffolds for bone regeneration [6, 7]. Noninvasive or minimally invasive surgery has been performed using cell micro-

carriers to heal specifically bone defects with irregular shape [8], which offers desirable advantages such as repair with minimal scarring, short operation times, reduced complications, and improvement in patient comfort and satisfaction [6, 9, 10]. Synthetic poly (γ-benzyl-L-glutamate) (PBLG) is one of synthetic polypeptides formed by a peptide bond linkage between the amino group on the carbon of one glutamic acid and the carboxyl group on the carbon of the next glutamic acid [11, 12].

In previous studies, we developed synthetic PBLG polypeptide microspheres with porous structure and good biocompatibility. Using this PBLG microspheres as injectable cellular carriers, we successfully generated cartilage as well as adipose-like tissue subcutaneously in nude mice [13, 14]. These results demonstrate that the PBLG porous microspheres possess great potential as injectable carriers for tissue engineering. However, whether this PBLG microspheres could be used in treating bony nonunions remains to be answered.

Immunoprivilege properties of ASCs have been well documented in a variety of studies including ours in which we demonstrated that allogeneic osteogenic differentiated ASCs maintain low immunogenicity and immunomodulation [15, 16]. Moreouve, it has been shown that allogeneic osteogenic differentiated ASCs combined with DBM successfully regenerate ulnar bone defects in rabbits without immunosuppressive therapies [16]. The use of allogeneic ASCs could meet clinical demand as an "off the shelf" product without waiting for expansion of autologous cells [17, 18]. In addition, the elderly could require cells with higher viability and differentiation potential from young healthy donors to heal bone defects and nonunions [19].

In the current study, we aimed to 1) investigate the attachment, proliferation, and osteogenic differentiation of ASCs within PBLG polypeptide microspheres; 2) evaluate the feasibility of using such a scaffold as injectable cellular carriers loading allogenic osteo-induced ASCs to heal bony nonunion in a mouse model.

Materials and methods

Preparation of PBLG porous microspheres

γ-benzyl-L-glutamate (BLG) was purchased from Sigma-Aldrich and used without further purication. BLG N-carboxyanhydride (BLG-NCA) was synthesized with slight modication according to our previous studies [20]. Dicyclohexylamine was purchased from Aladdin Reagent and puried by distillation before use. 1, 4-Dioxane and diethyl ether were purchased from Sinopharm Chemical Reagent, and 1, 4-dioxane was further distilled before use. Other chemicals were of analytical grade and used as received. PBLG microcarriers were prepared according to our previous study [13]. To investigate the morphology of the porous microcarriers, samples were sputter-coated with gold and examined under a scanning electron microscope (SEM; JSE-6500F, JEOL, Tokyo, Japan).

Cell culture and osteogenic differentiation

The experimental protocol was approved by the Animal Care and Experiment Committee of the Fudan University. ASCs were obtained from subcutaneous fat from the inguinal region of male, 3-week-old C57 mice. Adipose tissue was washed thoroughly with phosphate-buffered saline (PBS, pH 7.4) three times, finely minced, and digested in 0.075% type I collagenase (Washington Biochemical Corp, Lakewood, USA) at 37°C for 30 min. Enzyme activity was neutralized with low-glucose Dulbecco's modified Eagle's medium (LG-DMEM; Gibco, CA, USA), containing 10% fetal bovine serum (FBS; Gibco, CA, USA) as well as 100 μg/mL streptomycin + 100 U/mL penicillin (regular medium, GM). The solution was then centrifuged for 10 min at 1200 rpm. The cells were resuspended in the regular medium and plated at a density of $4 \times 10^4/cm^2$ in 60-mm culture dishes (Corning, NY, USA). The cells were maintained at 37°C in a humidified atmosphere containing 95% air and 5% CO_2. The medium was changed twice a week, and cells of passage 3 were collected for cell seeding.

For osteogenic differentiation, a different medium (OM) was used: It consisted of LG-DMEM with 10% FBS supplemented with 2 mM L-glutamine and 100 U/mL penicillin/1,000 U/mL streptomycin (all from Invitrogen, CA, USA), 0.01 μM 1,25-dihydroxyvitamin D3, 0.2 mM L-ascorbic acid-2-phosphate, and 10 mM β-glycerophosphate (all from Sigma, Taufkirchen, Germany). Cells were grown for a period of up to 14 days, and the medium was changed twice a week.

ASCs have previously demonstrated mesenchymal differentiation potential. Cells from passage 3 to 6 were stained for collagen type II (after chondrogenic differentiation; antibody:

ICN, Aurora, OH) as well as with ALP and Alizarin Red S (after osteogenic differentiation; Sigma, Taufkirchen, Germany) and with Oil red O staining (after adipogenic differentiation; Sigma, Taufkirchen, Germany). All stainings were performed according to the manufacturer's protocols.

Cell viability assays

Cell viability assays were performed using a cell-counting kit-8 (CCK-8 kit; Dojido, Japan). According to the manufacture's instruction, ASCs were seeded onto 96-well tissue culture polystyrene (TCPS) plates at a density of 1000 cells/well. Microspheres were placed onto each well with a density of 200/cm^2. For the control, ASCs cultured in wells without microspheres were used. The ASCs and microspheres were cultured at 37°C in a humidified atmosphere with 5.0% CO_2 for 1, 3, 5, and 7 days. At the endpoint, 20 μL CCK-8 (5 g/L) was added and incubated for 4 h. Finally, the absorbance was measured at 450 nm using the Victor3 microplate reader (Perkin-Elmer, MA, USA).

Cytotoxicity determination

The potential cytotoxicity of microspheres was assessed by measuring lactate dehydrogenase (LDH) leakage of ASCs into the culture medium by using a LDH-Cytotoxicity Assay Kit (Biovision, Mountain View, USA). Briefly, ASCs were seeded onto 48-well TCPS plates at a density of 6000 cells/cm^2. Microspheres were then placed onto each well with a density of 200/cm^2. For the control, ASCs cultured in wells without microspheres were used. The ASCs and microspheres were cultured at 37°C in a humidified atmosphere with 5.0% CO_2. After 1, 3, 5, and 7 days, the corresponding medium from each sample was collected for LDH-leakage measurement. Each well was then sonicated to estimate the intracellular LDH activity. The total LDH activity was calculated as the sum of the LDH activity in the medium and the intracellular LDH activity. The absorbance was measured spectrophotometrically at 490 nm against a reference filter set at 650 nm. The cytotoxicity of each sample was expressed as a percentage of the activity measured from the medium over that of the total LDH. Non-seeded wells treated similarly were used as blank controls, which were then subtracted from the corresponding samples.

Cell proliferation

To obtain the cell growth curve, 1 × 10^4 cells were seeded in a 12-well plate and cultured. Microspheres were placed onto each well with a density of 200/cm^2. ASCs cultured in wells without microspheres served as the control. Cell numbers of each well were counted at 1, 3, 5, and 7 days after seeding.

Seeding and growth of ASCs within PBLG microspheres

Before seeding, microspheres were sterilized by immersion in 75% ethanol for 30 min, followed by washing three times with PBS. In each flask, 1 × 10^7 ASCs were mixed with 60 mg microspheres in 10.0 mL DMEM with 20% FBS. To seed cells evenly on the microspheres, the flasks were shaken at 75 rpm for 6 h at 37°C in an incubator, following which 20.0 mL culture medium was added for long-term culture. Cell numbers within the microspheres were quantified at 1, 3, 5, and 7 days post-seeding by using a DNA assay. Briefly, the ASCs/microsphere mixture was lysed by repeated freeze-thawing and sonication cycles. After centrifugation at 10,000 rpm for 5 min, the supernatant was collected and the cell numbers were quantified using the Hoechst 33258 dye assay to measure the fluorescence intensity at an excitation wavelength of 365 nm and an emission wavelength of 460 nm. Extracellular matrix (ECM) deposition by ASCs within the microspheres was observed by SEM examination at 7 days after seeding.

Furthermore, to visualize the spatial distribution of ASCs within the microcarriers, ASCs were pre-labeled before seeding with fluorescent 3, 30-dioctadecyloxacarbocyanine perchlorate (DiO) dye (Molecular Probes, USA) at 37°C for 20 min according to the manufacturer's protocol. The labeled cells were then mixed with the microspheres. The cells grown within the microsphere were observed using a confocal laser microscope (Nikon Y-FL, Japan) at 7 days after seeding.

Osteogenesis of ASCs within PBLG microspheres

The osteogenic phenotype of ASCs with PBLG microspheres was determined by performing assays for ALP activity and accumulated calcium on days 4, 7, 10, and 14 post-seeding. Total RNA was extracted from cell layers using Trizol

Table 1. Sequences of Primers for qRT-PCR in the experiment

Gene	Primers (F=forward; R=reverse)
Runx2	F: 5'-GTCTTACCCCTCCTACCTGA-3'
	R: 5'-TGCCTGGCTCTTCTTACTGA-3'
ALP	F: 5'-ACGTGGCTAAGAATGTCATC-3'
	R: 5'-CTGGTAGGCGATGTCCTTA-3'
OCN	F: 5'-CAAAGGTGCAGCCTTTGTGTC-3'
	R: 5'-TCACAGTCCGGATTGAGCTCA-3'
β-actin	F: 5'-ATCATGTTTGAGACCTTCAA-3'
	R: 5'-CATCTCTTGCTCGAAGTCCA-3'

reagent (Invitrogen), according to the single-step acid-phenol guanidinium extraction method. The concentration of RNA was determined by measuring the optical absorbance at 260 nm. Thereafter, 1-5 μg of the extracted RNA samples was initially reversely transcribed for first-strand cDNA synthesis using a PrimeScript 1st Strand cDNA synthesis Kit (Takara, Daliang, China). Real-time PCR was performed in a T3 thermocycler (Biometra) using a quantitative real-time amplification system (MxPro-Mx3000P; Stratagene, CA, USA). SybrGreen PCR MasterMix (Applied Biosystems, CA, USA) was used in each reaction. Markers of osteogenic differentiation (*Runx2*, *ALP*, and *OCN*) were analyzed, and the β-actin housekeeping gene served as the control (sequences of primers, individual annealing temperatures, and amplicon lengths are shown in **Table 1**). Real-time expression of each gene of interest was calculated by normalizing the quantified cDNA transcript level (cycle threshold) to that of β-actin using the MxPro-Mx3000P system.

Surgical procedure

10-week-old (mean age) C57 mice were anesthetized by intraperitoneal injection of 400 mg/kg chloral hydrate. Under sterile conditions, a longitudinal incision of 4 mm was made just medial to the right patellar tendon, and the patella was dislocated laterally. Subsequently, a distally flattened 24 G needle was inserted from the trochlear groove into the femoral canal in a retrograde manner, and the pin at the right knee was cut appropriately. Thereafter, the middle of the femur was exposed through a lateral approach, and a 2-mm critical-sized defect was created in the middle of the femur using bone-cutting scissors. A custom-made clip of 8-mm length, made of a 27 G needle (Ø, 0.4 mm), was then implanted ventro-dorsally through the medullary cavity, just passing the intramedullar pin laterally. Finally, the wound was completely closed. Normal weight-bearing activities were allowed following the operation. After radiological non-union confirmation at 4 weeks, all animals underwent a second intervention. Under anesthesia, the segmental non-union was exposed through a small skin incision. The mice were then randomly divided into three groups. In one group (PBLG, n = 5), animals received local injection of PBLG suspended in 50 μL PBS. In the second group (ASCs/PBLG, n = 5), animals received local injection of ASCs cells (1×10^6) with PBLG suspended in 50 μL PBS. In the third group (PBS, n = 5), animals received local transplantation of the same volume of PBS. After 8 weeks, the animals were killed by cervical dislocation, and fracture healing was evaluated by radiological analysis and histological analysis.

Detection of systemic immunological reactions

To detect general immune rejection, 0.5 mL of blood was drawn from the caudal vein of each animal at selected time points postoperatively. The ratios of CD4-positive lymphocytes versus CD8-positive lymphocytes (CD4/CD8) were determined using flow cytometry analysis on days 0, 1, 3, 5, and 7. Serum contents of immune cytokines including interleukin (IL)-2, IL-4, and interferon (IFN)-γ were measured using enzyme-linked immunosorbent assay kits (Jiancheng Biotechnology Company, Nanjing, China) at weeks 0, 1, 2, 4, and 8 post-surgery according to the manufacturer's protocols.

Radiological analysis

At the end of the observation time, mice were re-anesthetized and ventro-dorsal radiography of the right femur was performed. Bone-defect regeneration was identified by the presence of bridging callus on 2 cortices. To read the image more clearly, we first removed the metallic clip.

Micro-computed tomography (micro-CT) evaluation

The micro-architecture of repaired bone was evaluated using SkyScan-1176 micro-computed tomography (μCT) (Bruker micro CT, Belgium). The settings used for image acquisition were as follows: 8.96 μm voxel size, 45 kV, 500 μA, and 0.5 degrees rotation step (180° angular range). For three-dimensional analysis, mi-

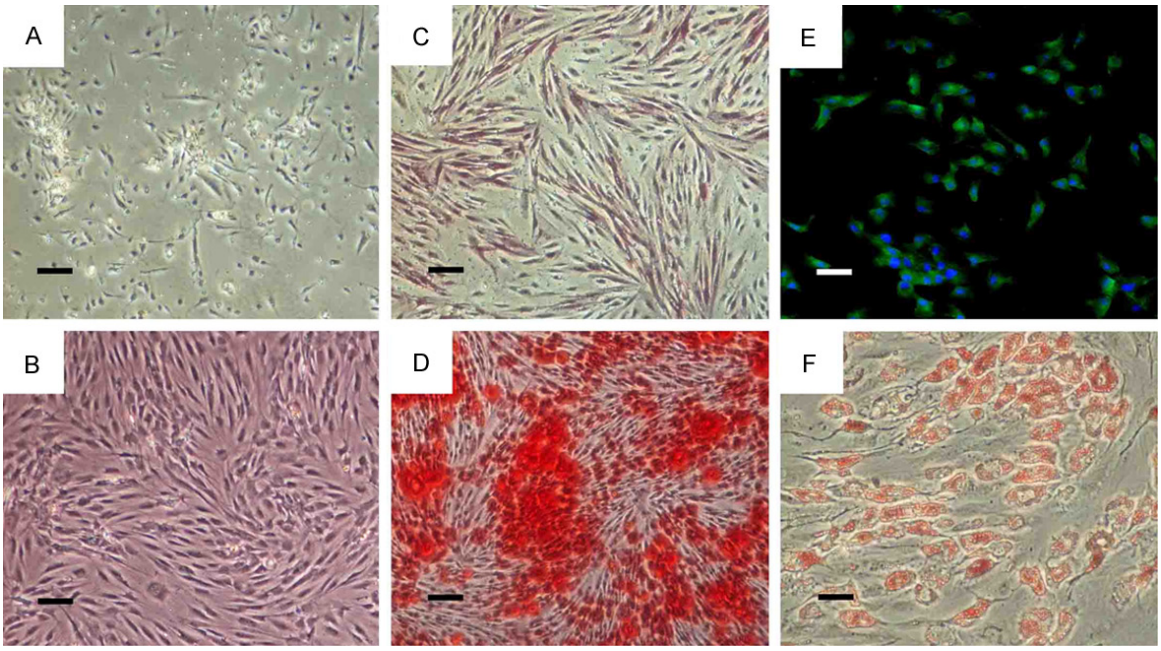

Figure 1. Morphology and multilineage differentiation of ASCs. ASCs of passages 0 and 3 exhibit fibroblast-like morphology (A & B, respectively). Osteogenic differentiation seen by positive ALP staining (C) and alizarin red staining (D). Chondrogenic differentiation for the presence of collagen type IIverified by immunofluorescence staining (E). Adipogenic differentiation confirmed by positive Oil Red O staining (F). Scale bars: 200 μm for (A); 100 μm for (B-D); and 50 μm for (E and F). ASC, adipose-derived stem cells; ALP, alkaline phosphatase.

cro-CT evaluation was performed on a 4-mm region centering on the point of fracture. The grey threshold for three-dimensional analysis ranged from 120 to 255.

Histological examination

Bone specimens were fixed in 4% neutral buffered formalin for 48 h and rinsed in tap water overnight. Thereafter, specimens were subjected to a quick decalcification with an agent containing 14% hydrochloric acid and subsequently rinsed with running tap water overnight. The tissues were then embedded in paraffin, sectioned in 5-μm thickness, and were stained with hematoxylin-eosin (H&E) and Azan-Mallory staining, respectively.

Statistical analysis

Paired Student's *t*-test was used for statistical analysis, and a P value < 0.05 was considered statistically significant.

Results

Culture and differentiation potential of ASCs

In the primary culture, ASCs isolated from subcutaneous fat of the inguinal region of male mice exhibited a relatively homogenous, fibroblast-like morphology (**Figure 1A**, **1B**), which could be expanded easily *in vitro*. During *in vitro* expansion using the osteogenic medium, osteogenic differentiation of ASCs was visualized by positive expression of ALP (**Figure 1C**) and calcified ECM deposition stained with Alizarin Red S (**Figure 1D**). Chondrogenic differentiation of ASCs was observed by immunofluorescence staining for the presence of collagen type II deposition (**Figure 1E**), and adipogenic differentiation was observed by intracellular accumulation of lipid droplets stained by Oil Red O (**Figure 1F**).

Evaluation of PBLG microspheres for compatibility of ASCs

PBLG microspheres fabricated from 6.5% gelatin exhibited an average pore diameter of 50.9-10.3 mm and a porosity of 86.58-2.37%, as observed by SEM (**Figure 2A**, **2B**).

Cellular viability and cytotoxicity between cells growing in microspheres and those cultured on TCP showed no significant difference after 1, 3, 5, and 7 days (**Figure 3A**, **3B**). In addition, cell number estimated by the DNA assay revealed no significant difference between cells growing

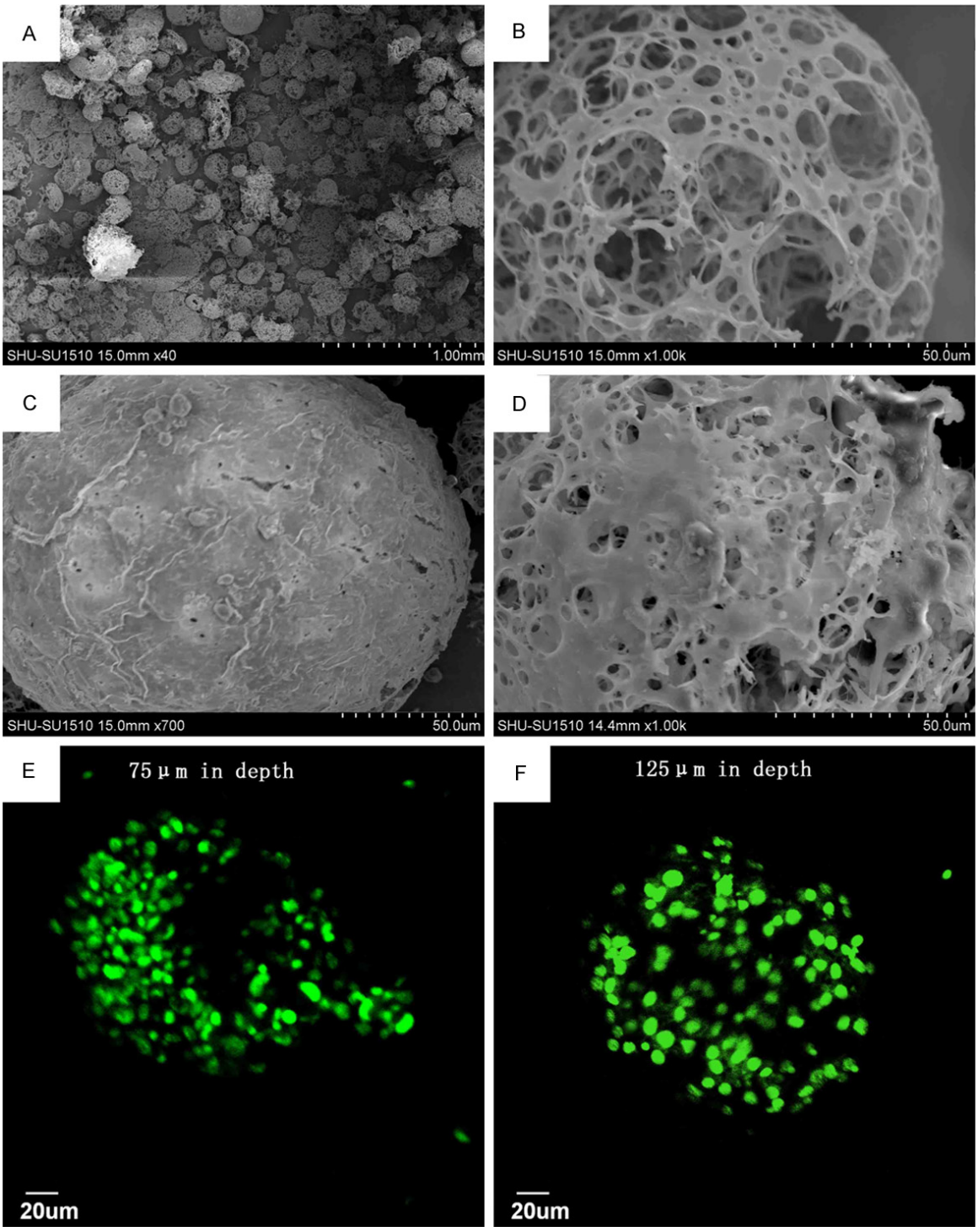

Figure 2. Physical characteristics of PBLG microspheres. SEM examination of the whole porous PBLG microspheres (A & B). Seven days after cell seeding, SEM shows large amounts of ECM deposition onto the PBLG microspheres (C & D). Confocal laser microscopy of DiO-labeled ASCs at the indicated depth in the microsphere after cell seeding for 7 days (E & F). PBLG, poly (γ-benzyl-L-glutamate); SEM, scanning electron microscope; ECM, extracellular matrix; DiO, 3, 30-dioctadecyloxacarbocyanine perchlorate.

with and those growing without PBLG microspheres (**Figure 3C**).

At 7 days after cell seeding, quantitative assays demonstrated that the ASCs proliferated rapid-

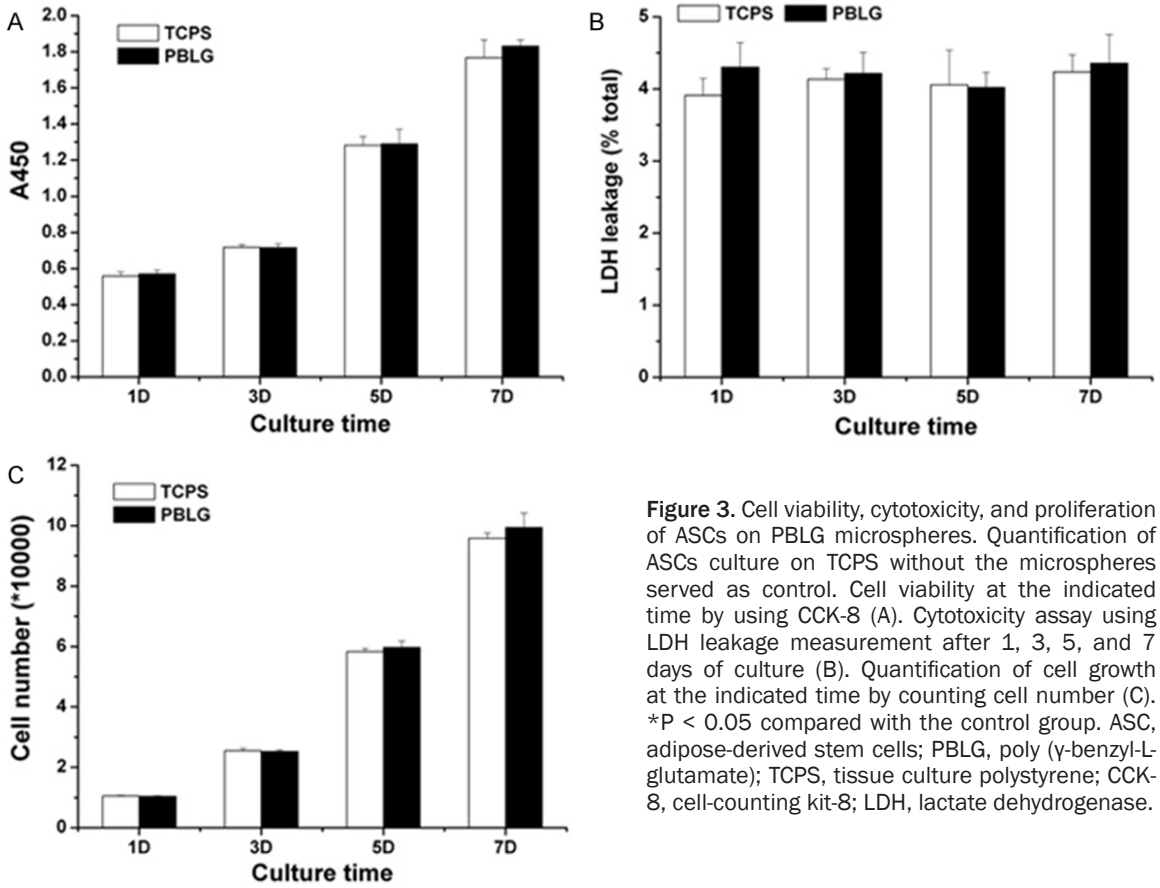

Figure 3. Cell viability, cytotoxicity, and proliferation of ASCs on PBLG microspheres. Quantification of ASCs culture on TCPS without the microspheres served as control. Cell viability at the indicated time by using CCK-8 (A). Cytotoxicity assay using LDH leakage measurement after 1, 3, 5, and 7 days of culture (B). Quantification of cell growth at the indicated time by counting cell number (C). *P < 0.05 compared with the control group. ASC, adipose-derived stem cells; PBLG, poly (γ-benzyl-L-glutamate); TCPS, tissue culture polystyrene; CCK-8, cell-counting kit-8; LDH, lactate dehydrogenase.

ly in the PBLG microspheres (**Figure 4A**). Moreover, SEM examination showed that ASCs attached well on the outer surface of PBLG microspheres and a good amount of extracellular matrix (ECM) was detected after culture for 7 days (**Figure 2C**, **2D**).

The presence of DiO-labeled ASCs assessed using a confocal microscope after cultivation for 7 days revealed that labeled ASCs were detected at 75 μm and 125 μm in depth respectively (**Figure 2E**, **2F**, respectively), suggesting that the ASCs occupied not only the surface but also the innermost region of the microspheres by gradually migrating inward to the inner region of PBLG microspheres.

Osteogenic differentiation of ASCs on PBLG microspheres

To address whether the ASCs grown in the PBLG microspheres could maintain their osteogenic phenotype, the expression of ALP and calcium accumulation were measured on days 4, 7, 10, and 14 post-seeding. We found that the expression of ALP in the osteo-differentiated group began to increase by day 7 and continued to increase through days 10 and 14 (**Figure 4B**). The amount of calcium accumulated by osteo-differentiated ASCs increased significantly by day 14 (**Figure 4C**). Both ALP expression and accumulated calcium in the undifferentiated group remained at a relatively constant low level throughout the study period. This result is further substantiated by the results of PCR for osteogenesis-related genes. The osteogenesis-related genes *Runx2*, *ALP*, and *OCN* were detected at high levels in the osteo-induced ASCs, indicating that these ASCs could maintain their osteogenic phenotype after seeding into PBLG microspheres (**Figure 5**). Because expression of ALP and accumulated calcium synergistically increased on day 14, cells/PBLG microspheres composites cultured *in vitro* for 14 days were chosen for subsequent *in vivo* implantation.

Detection of systemic immunological reactions

All the animals recovered from the surgical procedure rapidly without complications. During

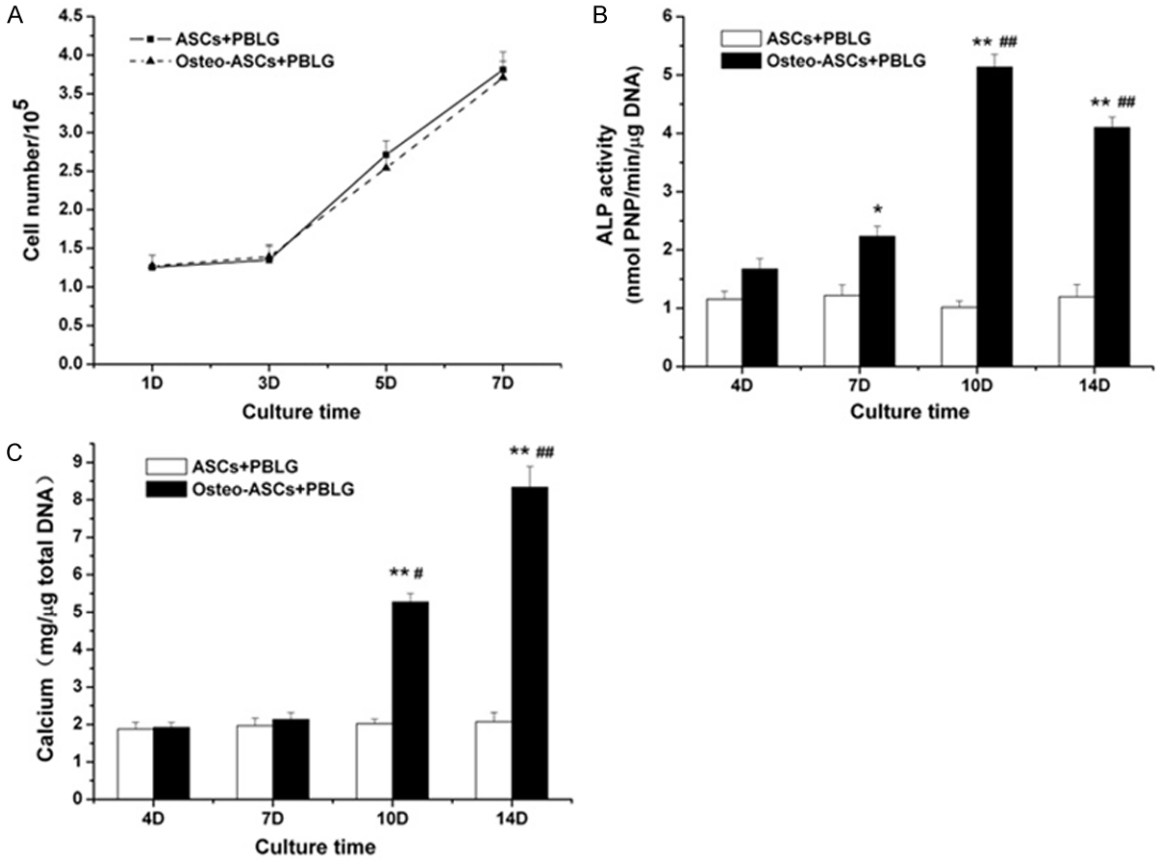

Figure 4. *In vitro* proliferation and characterization of osteo-differentiation of ASCs on PBLG microspheres. Proliferation of osteo-differentiated and undifferentiated ASCs on PBLG microspheres determined by DNA assay using Hoechst 33258 dye on days 1, 3, 5, and 7. PBLG microspheres alone cultured in osteogenic culture medium served as an empty (A). Osteogenic differentiation of osteo-differentiated and undifferentiated ASCs cultured on PBLG microspheres evaluated by the expression of ALP (B) and accumulated calcium (C) on days 4, 7, 10, and 14 post-seeding. PBLG microspheres seeded with undifferentiated ASCs served as a control. *P < 0.05 vs respective undifferentiated ASCs controls, **P < 0.01 vs undifferentiated ASCs controls, #P < 0.05 vs 4-day osteo-differentiated ASCs cultured with OM, ##P < 0.01 vs 4-day osteo-differentiated ASCs cultured with OM. ASC, adipose-derived stem cells; PBLG, poly (γ-benzyl-L-glutamate); ALP, alkaline phosphatase; OM, osteo-differentiated medium.

the observation period, no mice showed symptoms such as fever, infection, swelling, or implantation-site dehiscence. CD4/CD8 ratios on days 0, 1, 3, 5, and 7 post-surgery showed no statistically significant changes from that on day 0 (baseline value) (P > 0.05, **Figure 6A**). Moreover, the serum concentrations of IL-2, IL-4, and IFN-γ measured at postoperative weeks 1, 2, 4, and 8 showed no significant increase compared with the corresponding samples harvested at week 0 (P > 0.05, **Figure 6B-D**).

Radiographic evaluation of fracture healing

X-ray images revealed that none of the femurs in any of the groups demonstrated healing 8 weeks after operation (**Figure 7A**), and no internal fixation failure was observed in any mice. Mice in the PBS group and the PBLG group remained unhealed (**Figure 7B**, **7C**). However, in the ASCs/PBLG group, the femoral segmental defect was occupied by newly formed bone (**Figure 7D**).

Micro-CT evaluation

Three-dimensional micro-CT scanning was used to evaluate repair of the femoral non-union at 8 weeks post-surgery. The femoral non-union treated with PBS or PBLG alone had less repair at 8 weeks post-surgery, while the femoral nonunions that were treated with the ASCs/PBLG composite were almost completely repaired at 8 weeks post-surgery (**Figure 8**).

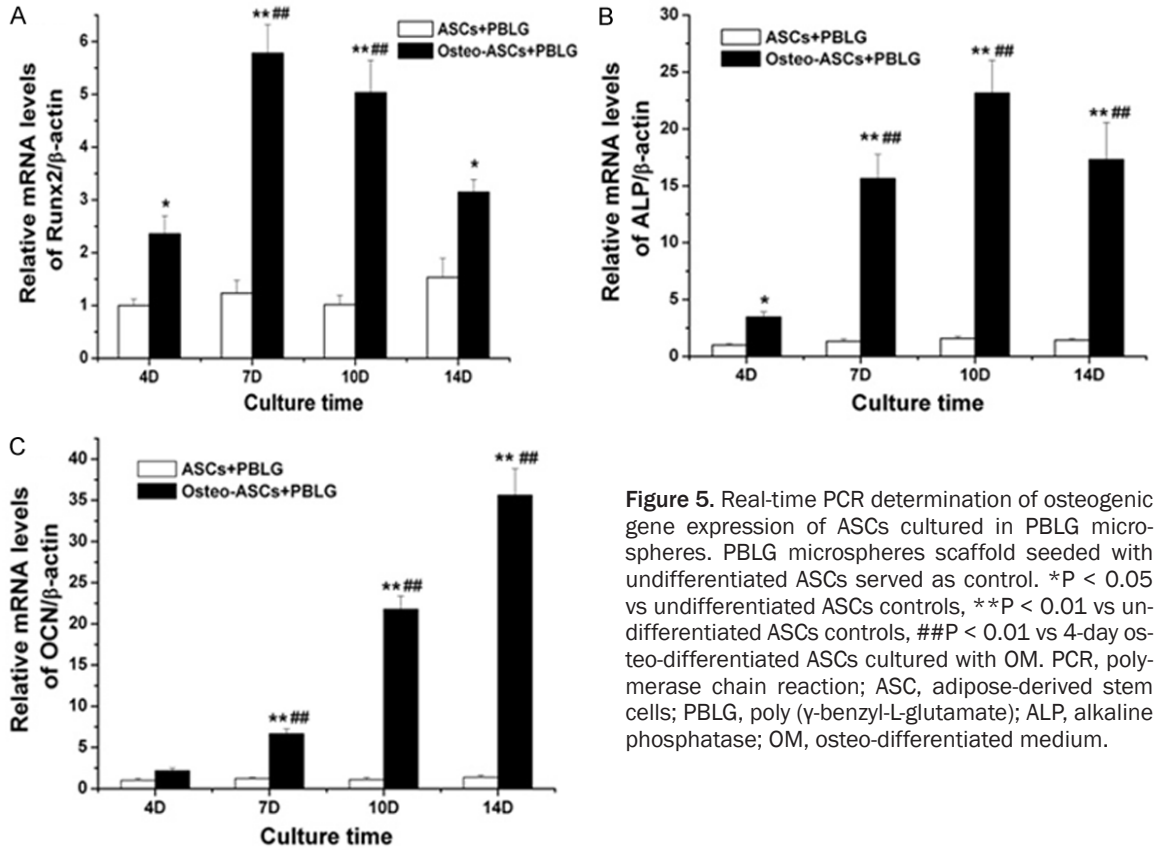

Figure 5. Real-time PCR determination of osteogenic gene expression of ASCs cultured in PBLG microspheres. PBLG microspheres scaffold seeded with undifferentiated ASCs served as control. *P < 0.05 vs undifferentiated ASCs controls, **P < 0.01 vs undifferentiated ASCs controls, ##P < 0.01 vs 4-day osteo-differentiated ASCs cultured with OM. PCR, polymerase chain reaction; ASC, adipose-derived stem cells; PBLG, poly (γ-benzyl-L-glutamate); ALP, alkaline phosphatase; OM, osteo-differentiated medium.

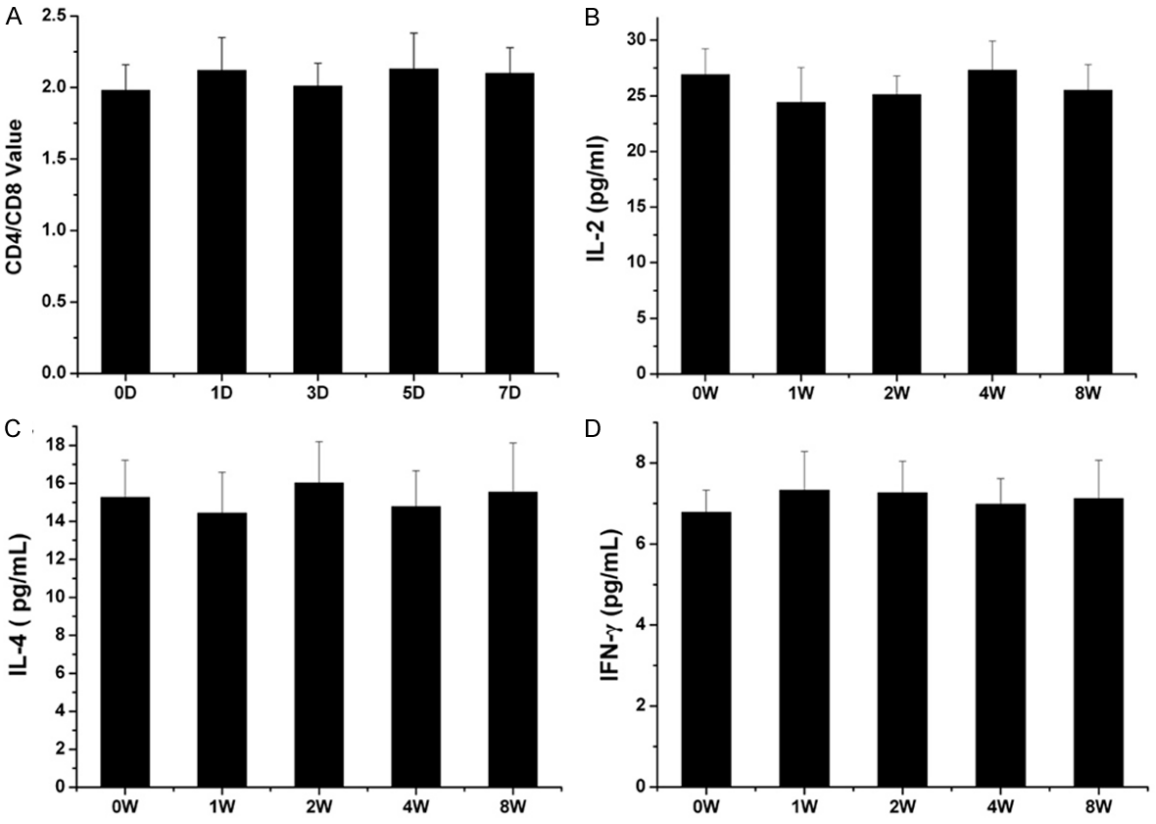

Figure 6. Detection of systemic immunological reactions after allogeneic ASCs transplantation. (A) Flow cytometric analysis shows no significant changes in the CD4/CD8 ratios on postoperative days 1, 3, 5, and 7 compared with those on day 0 (n = 5, P > 0.05). The serum concentrations of IL-2 (B), IL-4 (C), and INF-γ (D) measured at 1, 2, 4, and 8 weeks after surgery, and no significant differences are detected compared to the corresponding values on week 0 (n = 5, P > 0.05). ASC, adipose-derived stem cells; IL, interleukin; INF, interferon.

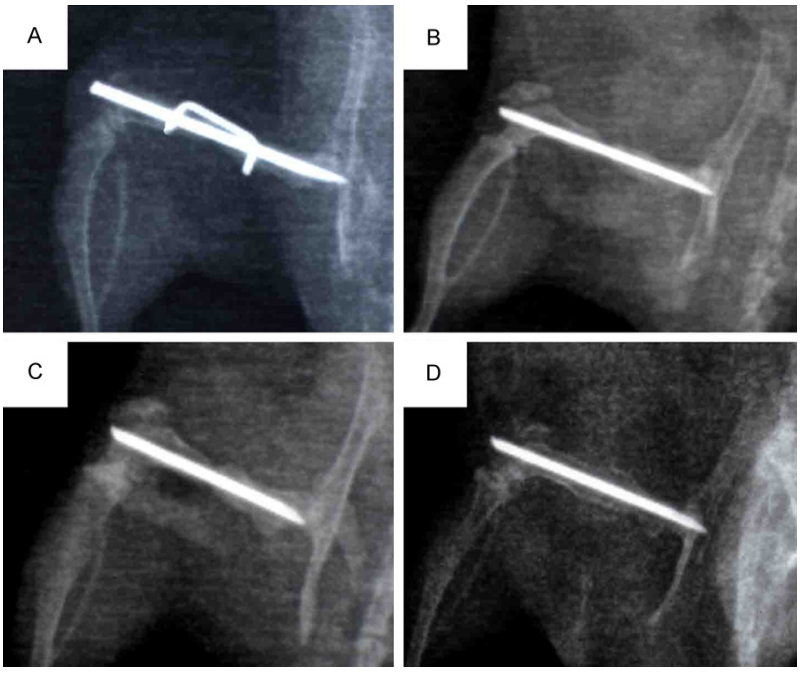

Figure 7. Representative radiographs of the right femur at 8 weeks after creating a segmental non-union. (A) Non-union treated with PBS (B) and PBLG microspheres (C) remain unhealed, whereas non-union treated with ASCs/PBLG microspheres (D) are occupied by newly formed bone. PBS, phosphate-buffered saline; ASC, adipose-derived stem cells; PBLG, poly (γ-benzyl-L-glutamate).

The coronal transverse-sectional analyses of the non-union sites demonstrated that non-union treated with PBS or PBLG alone were not repaired and connected by bone regeneration, whereas the non-union treated with ASCs/PBLG composites were repaired and connected structurally by tissue-engineered bone (**Figure 8D-F**). In addition, a statistically significant increase in bone volume (BV) and bone volume/total volume ratio (BV/TV) were detected between non-union treated with PBS or PBLG alone and that treated with ASCs/PBLG (**Figure 8G**, **8F**). Furthermore, a statistically significant decrease in trabecular pattern factor (Tb.Pf) was detected between non-union treated with PBS or PBLG alone and that treated with ASCs/PBLG (**Figure 8I**).

Histological examination

At 8 weeks post-implantation, H&E staining showed that there was no bridging bone formation within non-union site in the PBS and PBLG-alone groups, and the non-union of the femur was filled with loose fibrous tissue (**Figure 9A-F**). In the ASCs/PBLG group, regenerated bone showing typical structure of mature trabecula as well as re-connected marrow cavity was observed. Moreover, some small clusters of chondrogenic-like cells were observed be scattered in the neo-generate bone tissues, indicating a process of endochondral bone formation occurred during repair of non-union bone (**Figure 9G-I**). In addition, Azan-Mallory staining showed that new bone tissue (red staining) regenerated the non-union in the ASCs/PBLG group (**Figure 10**).

Discussion

Bone non-union is a frequent complication in surgical treatment of fractures and remains a major challenge for orthopedic surgery [1, 3]. Many strategies have been used in the treatment of non-union, among which, bone autograft represents the gold standard therapeutic approach [1, 21]. However, autograft bone is associated with several disadvantages such as donor-site morbidity and lack of supply, which limit its clinical use [3, 5]. Allografts, on the other hand, feature good osteo-conductive properties but carry a risk of disease transmission [22]. The rapid development of bone tissue engineering provides an attractive approach for the treatment of non-union, by which functional new bone tissue is generated in non-union site with the combination of seed cells and bio-scaffolds [23]. In the last decade, well-designed and porous three-dimensional biodegradable scaffolds that provide a large surface area for cell attachment and proliferation and guide tissue formation have gained importance

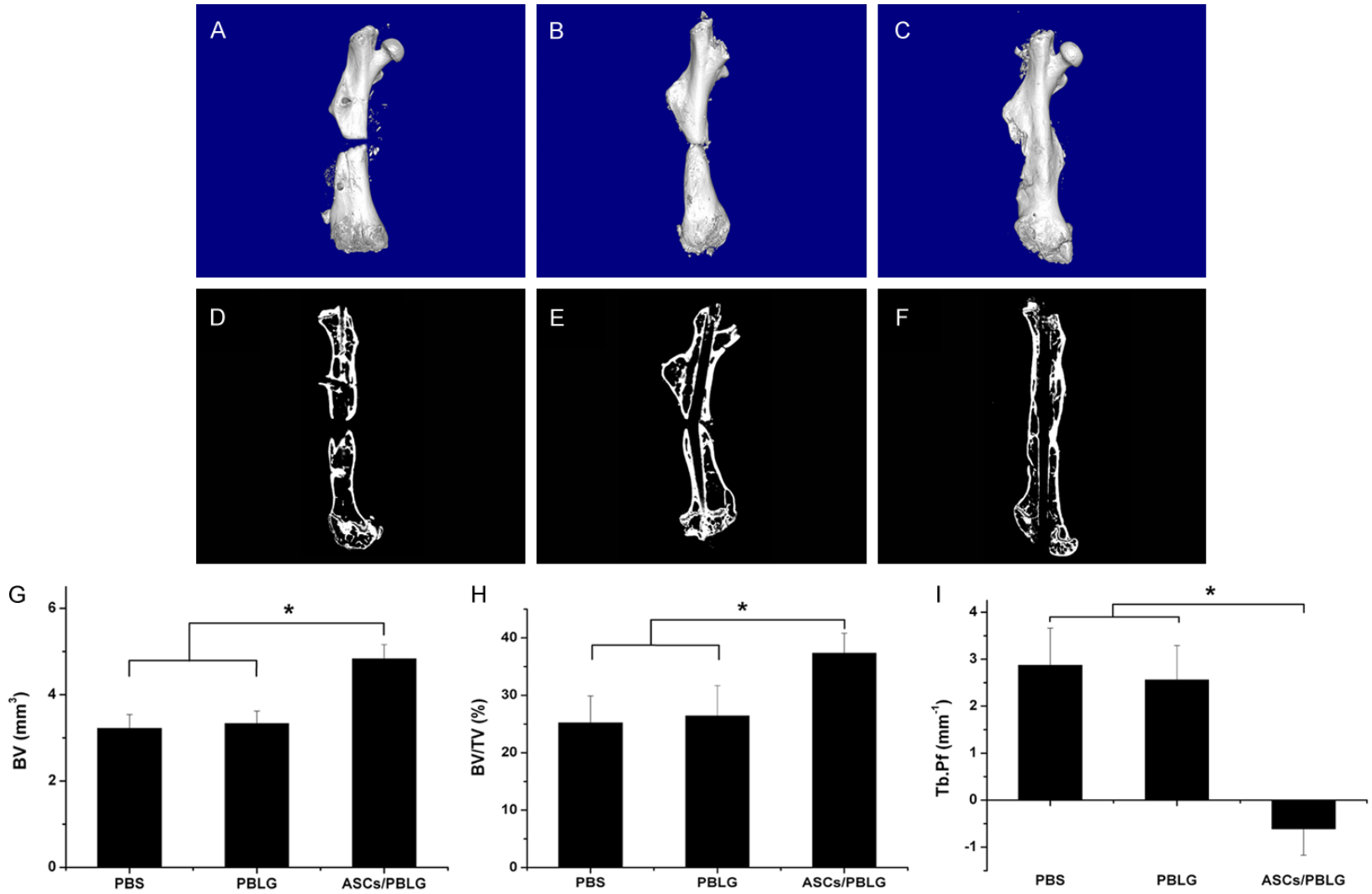

Figure 8. Micro-CT evaluation of femoral bone repair at 8 weeks post-implantation. Three-dimensional reconstruction of the actual non-union sites shows that at the PBS-treated site or PBLG microspheres-treated site (A & B), the non-union are left unconnected. At ASCs/PBLG microspheres composite-treated sites (C), the tissue-engineered bone is connected with the surrounding normal bone. The coronal transverse sectional analyses confirms the observation of three-dimensional reconstruction (D-F). Structure parameter bone volume (BV), bone volume/total volume ratio (BV/TV) and trabecular pattern factor (Tb.Pf) were measured by micro-CT (G-I). CT, computed tomography; PBS, phosphate-buffered saline; ASC, adipose-derived stem cells; PBLG, poly (γ-benzyl-L-glutamate).

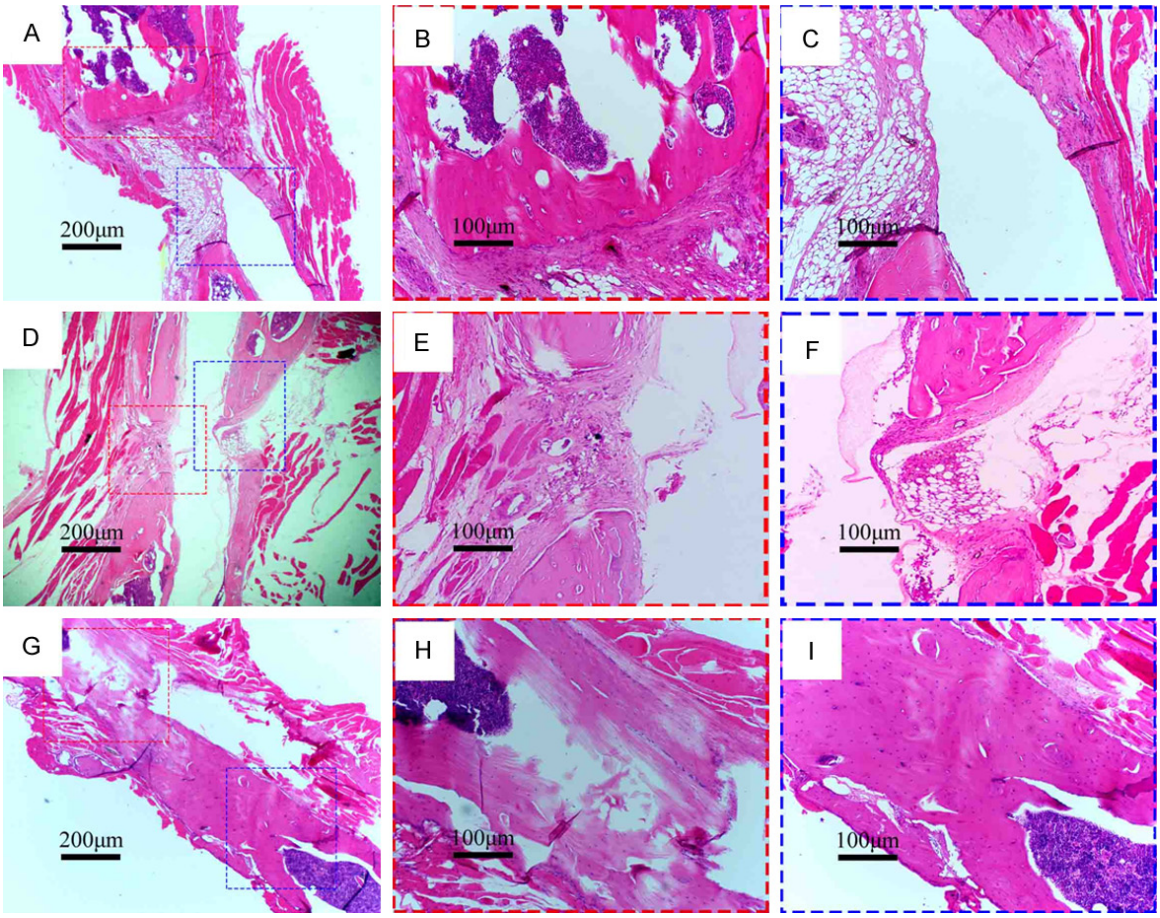

Figure 9. H&E staining evaluation at 8 weeks post-implantation. H&E staining shows that the PBS-treated or PBLG microspheres-treated non-union (A-F) is filled with loose fibrous tissue, whereas the ASCs/PBLG microspheres composite-treated non-union is filled with mature bone structure (G-I). H&E, hematoxylin-eosin; PBS, phosphate-buffered saline; ASC, adipose-derived stem cells; PBLG, poly (γ-benzyl-L-glutamate).

in bone tissue-engineering [10]. However, transplantation of these spongy scaffolds needs an open surgery and is not suitable for repairing irregularly shaped bone defects and nonunions. Thus, injectable scaffolds hold more potential in regeneration of non-union and bone defects owing to their advantages such as ability to maintain cell differentiated phenotype and repair irregularly shaped defect, ease of operation using needle syringes, and shorter operative times [24, 25].

Injectable porous microspheres have been designed from synthetic polymers such as chitosan and poly (lactic-co-glycolic acid) for bone tissue engineering [10, 26, 27]. However, most injectable porous microspheres have been fabricated from the aliphatic polyesters and their derivatives usually, leading to local inflammatory reactions *in vivo* [13]. Synthetic polypeptides originate from a wide choice of a-amino acid monomers linked with peptide bonds and thus mimic natural proteins. Compared to synthetic aliphatic polyesters and polycarbonates, synthetic polypeptides are considered a more reasonable material for tissue engineering because of their several practical advantages, such as the inherent ability to biodegrade into non-toxic products with a near-neutral pH, signicant functionality, good biocompatibility, and nonimmunogenicity [11-13, 28]. Previous studies by ours and others found that polypeptides-synthetic PBLG-can be eventually degraded into monomer units of L-glutamic acid, an important component of the body tithout eliciting harmful inflammatory reactions [11, 12]. Furthermore, synthetic PBLG and its derivatives have been developed as implantable scaffolds for bone tissue engineering [29], showing good biocompatibility and osteogenesis capacity in

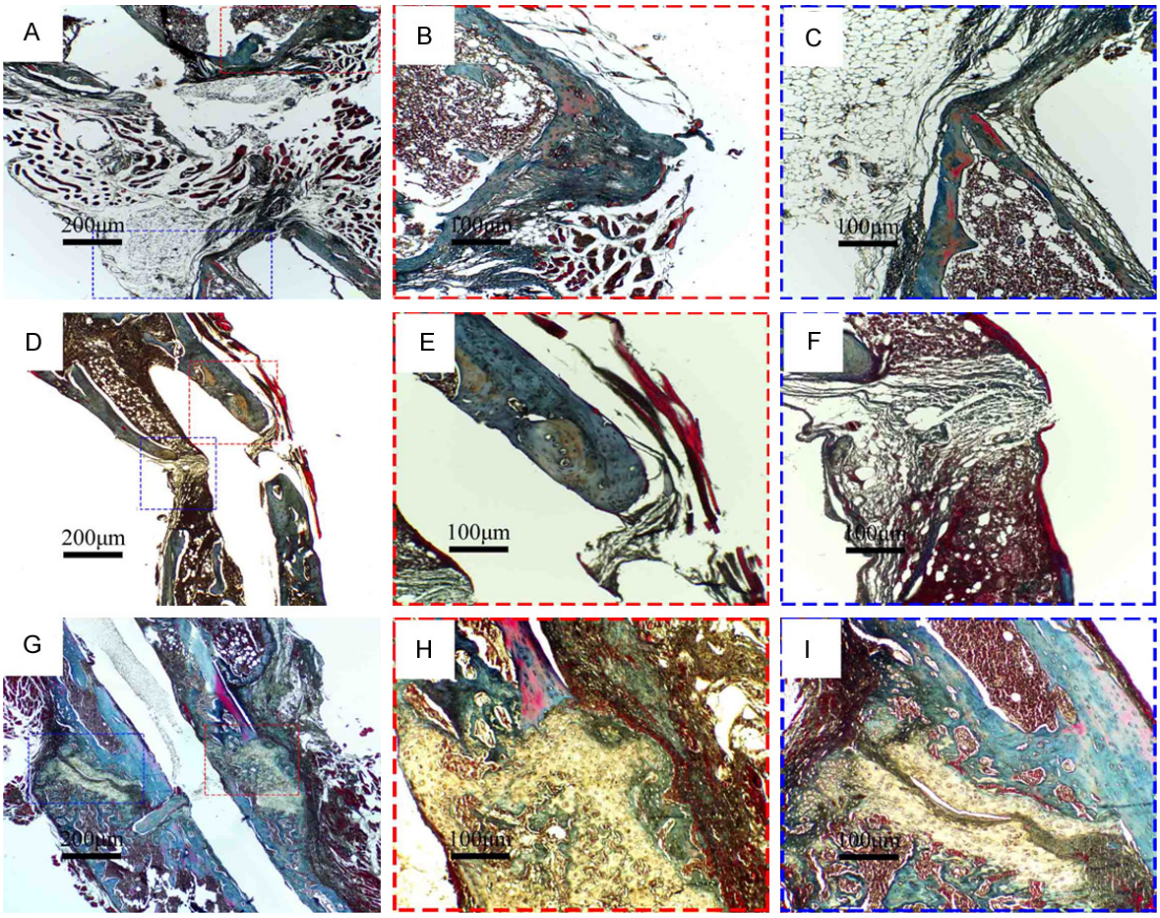

Figure 10. Azan-Mallory staining evaluation at 8 weeks post-implantation. Azan-Mallory staining shows that new bone tissue (red staining) and fibrous tissue (blue staining) fill the ASCs/PBLG microspheres composite-treated non-union (G-I), whereas no bone tissue is observed in non-union treated with PBS-treated or PBLG microspheres only (A-F). PBS, phosphate-buffered saline; ASC, adipose-derived stem cells; PBLG, poly (γ-benzyl-L-glutamate).

vivo. Using fabricated porous microspheres from the synthetic PBLG, we successfully constructed tissue-engineered cartilage and adipose via subcutaneous injection of PBLG microsphere-loaded chondrocytes and adipogenic ASCs into nude mice, respectively [13, 14]. The PBLG porous microspheres fabricated in our studies showed controllable degradation properties and good cytocompatibility for utilization as an injectable vehicle for tissue engineering. Therefore, in this study, we investigated the attachment, proliferation, and osteogenic differentiation of ASCs in PBLG microspheres and explored the feasibility of applying PBLG microspheres as an injectable vehicle to repair femoral non-union in a mice model.

An ideal bio-scaffold must exhibit good biocompatibility for the seeded cells. In the current study, the CCK-8, LDH, and cell-number assays showed no significant difference in cellular viability, cytotoxicity, and proliferation between cells growing in PBLG microspheres and those cultured on TCP after 1, 3, 5, and 7 days. Thus, the PBLG microspheres exhibited favorable biocompatibility with the seeded ASCs.

Adhesion and proliferation of seed cells on microspheres indicate the occurrence of cell-material interaction and influence the processes of seed cells including differentiation, ECM deposition, and maturation. Consequently, we seeded ASCs in PBLG microspheres and cellular proliferation was observed. The quantitative assay revealed a significantly elevated cellular proliferation in 7 days of cultivation, indicating that the PBLG microspheres possessed good biocompatibility to support the proliferation of ASCs *in vitro*. Consistent with the quantitative assay of proliferation, the images observed by SEM showed that ASCs attached well on the PBLG microspheres and abundant ECM was

deposited in the microspheres on day 7. Furthermore, the images observed by confocal microscope showed that a significant number of DiO-labeled ASCs migrated inside the PBLG microspheres, which indicated that the pore size as well as interconnection of pores in PBLG microspheres was generally suitable for ASCs to adhere and migrate into the inner pores.

Osteogenesis of ASCs seeded in the PBLG microspheres is one of the key issues determining the success of bone generation in vivo. In this study, we detected ALP expression and extracellular deposition of calcium to evaluate osteogenesis of ASCs seeded. ALP is considered a key enzyme that control earl osteogenesis by regulating organic or inorganic phosphate metabolism via the hydrolysis of phosphate esters, and functions as a plasma-membrane transporter for inorganic phosphates [30]. The extracellular deposition of calcium was a marker expressed in late osteogenesis, which indicated osteogenesis maturation [31]. ASCs seeded in microspheres were shown to express high-level ALP and calcium in the duration of 2 weeks. Consistent with the results of the quantitative ALP and calcium deposition assays, expression of osteogenesis-related genes such as *Runx2, ALP,* and *OCN* initially increased on day 7 and reached a peak on day 10 after seeding. These data indicate that the PBLG microspheres help to retain the osteogenesis of ASCs *in vitro*.

Our previous study demonstrated that allogeneic osteogenic differentiated ASCs maintained low immunogenicity and negative immunomodulation. Furthermore, we successfully regenerated ulnar non-union in rabbits using allogeneic osteogenic differentiated ASCs combined with DBM without immunosuppressive therapies [24]. Therefore, in this study, we repaired the segment femoral defect in mice using allogeneic osteogenic differentiated ASCs-loaded PBLG microspheres to determine whether the PBLG microspheres prepared from PBLG could serve as injectable carriers for bone tissue engineering *in vivo*. The IL-2, IL-4, and INF-γ levels in serum after surgery showed no statistically significant difference compared to that on day 0, which indicated there was no immunological disturbance after allograft of engineered bone constructed with ASCs.

Radiological analyses revealed that femoral non-union that were treated with the ASCs/PBLG composite were almost completely repaired at 8 weeks post-surgery. However, the femoral non-union treated with PBS or PBLG alone showed a lower degree of repair at 8 weeks post-surgery. Histological analysis revealed that the ASCs/PBLG microsphere composite repaired the segment femoral non-union in mice with no ectopic neoformation, overgrowth, related immune response, or local inflammation in bone repairing site.

Despite our important findings, this study has a few limitations that need to be addressed. First, the biomechanical strength of the injectable engineered bone composed of PBLG porous microsphere and ASCs is poorer than that of the solid scaffolds. Therefore, rigid internal and/or external fixation was necessary during the repair surgery. Second, the injectable PBLG microsphere discussed in this study could not be used for infected non-union or non-union coexisting with other superficial infection of skin tissue. Finally, some non-union lead to complications and cause limb deformity, in which case, injection therapy cannot reconstruct the deformed limb until an operation is performed. Further study to promote the clinical application of injectable microspheres is therefore required.

Conclusion

The current study showed that ASCs attached, spread, and showed good osteogenic differentiation on the PBLG microspheres *in vitro*. The PBLG microspheres with osteogenic ASCs successfully repaired femoral non-union in mouse models *in vivo*. Therefore, the PBLG microspheres are potentially useful as an injectable vehicle for bone tissue engineering.

Acknowledgements

This work was financially supported by the Natural Science Foundation of China [grant number 81301335, 81471798], the Shanghai Municipal Commission of Health and Family Planning Foundation [grant number 20144037], and Beijing Yangfan Project (XMLX201611).

Disclosure of conflict of interest

None.

Address correspondence to: Jingbo Yin, Department of Polymer Materials, Shanghai University, Shanghai

200444, China. Tel: +86-21-63138341; Fax: +86-21-53078128; E-mail: jbyin@shu.edu.cn; Lei Cui, Department of Plastic Surgery, Beijing Shijitan Hospital Affiliated to Capital Medical University, Beijing 100038, China. E-mail: cuileite@aliyun.com

References

[1] Orth M, Kruse NJ, Braun BJ, Scheuer C, Holstein JH, Khalil A, Yu X, Murphy WL, Pohlemann T, Laschke MW and Menger MD. BMP-2-coated mineral coated microparticles improve bone repair in atrophic non-unions. Eur Cell Mater 2017; 33: 1-12.

[2] Megas P. Classification of non-union. Injury 2005; 36 Suppl 4: S30-37.

[3] Buza JA 3rd and Einhorn T. Bone healing in 2016. Clin Cases Miner Bone Metab 2016; 13: 101-105.

[4] Kanczler JM and Oreffo RO. Osteogenesis and angiogenesis: the potential for engineering bone. Eur Cell Mater 2008; 15: 100-114.

[5] Dimitriou R, Mataliotakis GI, Angoules AG, Kanakaris NK and Giannoudis PV. Complications following autologous bone graft harvesting from the iliac crest and using the RIA: a systematic review. Injury 2011; 42 Suppl 2: S3-15.

[6] Liu X, Jin X and Ma PX. Nanofibrous hollow microspheres self-assembled from star-shaped polymers as injectable cell carriers for knee repair. Nat Mater 2011; 10: 398-406.

[7] Man Y, Wang P, Guo Y, Xiang L, Yang Y, Qu Y, Gong P and Deng L. Angiogenic and osteogenic potential of platelet-rich plasma and adipose-derived stem cell laden alginate microspheres. Biomaterials 2012; 33: 8802-8811.

[8] Munarin F, Petrini P, Bozzini S and Tanzi MC. New perspectives in cell delivery systems for tissue regeneration: natural-derived injectable hydrogels. J Appl Biomater Funct Mater 2012; 10: 67-81.

[9] Liao J, Wang B, Huang Y, Qu Y, Peng J and Qian Z. Injectable alginate hydrogel cross-linked by calcium gluconate-loaded porous microspheres for cartilage tissue engineering. ACS Omega 2017; 2: 443-454.

[10] Kim SE, Yun YP, Shim KS, Park K, Choi SW, Shin DH and Suh DH. Fabrication of a BMP-2-immobilized porous microsphere modified by heparin for bone tissue engineering. Colloids Surf B Biointerfaces 2015; 134: 453-460.

[11] Li C. Poly(L-glutamic acid)--anticancer drug conjugates. Adv Drug Deliv Rev 2002; 54: 695-713.

[12] Song Z, Yin J, Luo K, Zheng Y, Yang Y, Li Q, Yan S and Chen X. Layer-by-layer buildup of poly(L-glutamic acid)/chitosan film for biologically active coating. Macromol Biosci 2009; 9: 268-278.

[13] Fang J, Yong Q, Zhang K, Sun W, Yan S, Cui L and Yin J. Novel injectable porous poly([gamma]-benzyl-l-glutamate) microspheres for cartilage tissue engineering: preparation and evaluation. Journal of Materials Chemistry B 2015; 3: 1020-1031.

[14] Sun W, Fang J, Yong Q, Li S, Xie Q, Yin J and Cui L. Subcutaneous construction of engineered adipose tissue with fat lobule-like structure using injectable poly-benzyl-L-glutamate microspheres loaded with adipose-derived stem cells. PLoS One 2015; 10: e0135611.

[15] Cui L, Yin S, Liu W, Li N, Zhang W and Cao Y. Expanded adipose-derived stem cells suppress mixed lymphocyte reaction by secretion of prostaglandin E2. Tissue Eng 2007; 13: 1185-1195.

[16] Gu H, Xiong Z, Yin X, Li B, Mei N, Li G and Wang C. Bone regeneration in a rabbit ulna defect model: use of allogeneic adipose-derivedstem cells with low immunogenicity. Cell Tissue Res 2014; 358: 453-464.

[17] O'Keefe RJ and Mao J. Bone tissue engineering and regeneration: from discovery to the clinic--an overview. Tissue Eng Part B Rev 2011; 17: 389-392.

[18] Liu G, Zhang Y, Liu B, Sun J, Li W and Cui L. Bone regeneration in a canine cranial model using allogeneic adipose derived stem cells and coral scaffold. Biomaterials 2013; 34: 2655-2664.

[19] Ren ML, Peng W, Yang ZL, Sun XJ, Zhang SC, Wang ZG and Zhang B. Allogeneic adipose-derived stem cells with low immunogenicity constructing tissue-engineered bone for repairing bone defects in pigs. Cell Transplant 2012; 21: 2711-2721.

[20] Xiao C, Zhao C, He P, Tang Z, Chen X and Jing X. Facile synthesis of glycopolypeptides by combination of ring-opening polymerization of an alkyne-substituted n-carboxyanhydride and click "glycosylation". Macromol Rapid Commun 2010; 31: 991-997.

[21] Soucacos PN, Dailiana Z, Beris AE and Johnson EO. Vascularised bone grafts for the management of non-union. Injury 2006; 37 Suppl 1: S41-50.

[22] Calori GM, Albisetti W, Agus A, Iori S and Tagliabue L. Risk factors contributing to fracture non-unions. Injury 2007; 38 Suppl 2: S11-18.

[23] Quarto R and Giannoni P. Bone tissue engineering: past-present-future. Methods Mol Biol 2016; 1416: 21-33.

[24] Fang J, Zhang Y, Yan S, Liu Z, He S, Cui L and Yin J. Poly(L-glutamic acid)/chitosan polyelectrolyte complex porous microspheres as cell microcarriers for cartilage regeneration. Acta Biomater 2014; 10: 276-288.

[25] Kim SE, Yun YP, Shim KS, Park K, Choi SW and Suh DH. Effect of lactoferrin-impregnated porous poly(lactide-co-glycolide) (PLGA) microspheres on osteogenic differentiation of rabbit adipose-derived stem cells (rADSCs). Colloids Surf B Biointerfaces 2014; 122: 457-464.

[26] Tao C, Huang J, Lu Y, Zou H, He X, Chen Y and Zhong Y. Development and characterization of GRGDSPC-modified poly(lactide-co-glycolide acid) porous microspheres incorporated with protein-loaded chitosan microspheres for bone tissue engineering. Colloids Surf B Biointerfaces 2014; 122: 439-446.

[27] Shen S, Fu D, Xu F, Long T, Hong F and Wang J. The design and features of apatite-coated chitosan microspheres as injectable scaffold for bone tissue engineering. Biomed Mater 2013; 8: 025007.

[28] Xing T, Lai B, Ye X and Yan L. Disulfide core cross-linked PEGylated polypeptide nanogel prepared by a one-step ring opening copolymerization of N-carboxyanhydrides for drug delivery. Macromol Biosci 2011; 11: 962-969.

[29] Qian J, Yong X, Xu W, Jin X. Preparation and characterization of bimodal porous poly(γ-benzyl-L-glutamate) scaffolds for bone tissue engineering. Mater Sci Eng C Mater Biol Appl 2013; 33: 4587-93.

[30] Hessle L, Johnson KA, Anderson HC, Narisawa S, Sali A, Goding JW, Terkeltaub R and Millan JL. Tissue-nonspecific alkaline phosphatase and plasma cell membrane glycoprotein-1 are central antagonistic regulators of bone mineralization. Proc Natl Acad Sci U S A 2002; 99: 9445-9449.

[31] Liu H, Liu Y, Viggeswarapu M, Zheng Z, Titus L and Boden SD. Activation of c-Jun NH(2)-terminal kinase 1 increases cellular responsiveness to BMP-2 and decreases binding of inhibitory Smad6 to the type 1 BMP receptor. J Bone Miner Res 2011; 26: 1122-1132.